Environmental Engineering Research

Environ. Eng. Res. 2014 March,19(1) : 107-113

Research Paper

http://dx.doi.org/10.4491/eer.2014.19.1.107
pISSN 1226-1025 eISSN 2005-968X

Immobilized Small Sized Manganese Dioxide Sand in the Remediation of Arsenic Contaminated Water

Diwakar Tiwari[1], C. Laldawngliana[2], Seung-Mok Lee[3†]

[1]*Department of Chemistry, School of Physical Sciences, Mizoram University, Aizawl, Mizoram 96004, India*
[2]*Chemistry Department, Government Champhai College, Champhai, Mizoram 796321, India*
[3]*Department of Environmental Engineering, Kwandong University, Gangneung 210-701, Korea*

Abstract

Small sized manganese dioxide particles are immobilized onto the surface of sand by the wet impregnation process. The surface morphology of the solid, i.e., immobilized manganese dioxide natural sand (IMNS) is performed by taking scanning electron microscope images and characterized by the X-ray diffraction data. The specific surface area of the solid is obtained, which shows a significant increase in the specific surface area obtained by the immobilization of manganese dioxide. The pH_{PZC} (point of zero charge) is found to be 6.28. Further, the IMNS is assessed in the removal of As(III) and As(V) pollutants from aqueous solutions under the batch and column operations. Batch reactor experiments are conducted for various physicochemical parametric studies, viz. the effect of sorptive pH (pH 2.0–10.0), concentration (1.0–25.0 mg/L), and background electrolyte concentrations (0.0001–0.1 mol/L $NaNO_3$). Further, column experiments are conducted to obtain the efficiency of IMNS under dynamic conditions. The breakthrough data obtained by the column experiments are employed in non-linear fitting to the Thomas equation, so as to estimate the loading capacity of the column for As(III) and As(V).

Keywords: As(III), As(V), Column, Immobilized manganese dioxide natural sand (IMNS), pH, Sorption

1. Introduction

Water is an important and essential component of living being, but is increasingly becoming polluted day-by-day. Water quality requires an ongoing evaluation and revision at all levels (international, down to individual aquifers and wells). It was observed that the use of a deleterious quality of water caused several diseases [1]. The contamination of surface/ground waters by heavy metal toxic ions is a serious environmental and public concern, because of the known fact that these ions are virtually non-biodegradable and tend to accumulate within the biosystem causing various biological disorders [2]. Increased use of heavy metal toxic ions in various industrial processes led to the significant contamination of our aquatic environment. Besides the toxic and harmful effects to aquatic life, the extended perseverance of these pollutants in the biological systems and accumulation in the biosphere through the food chain resulted in environmental and occupational hazards [3, 4].

Arsenic is generally found as a contaminant in soil and water systems due to various anthropogenic sources, geologic variance, arsenic mine drenching, and dissolution of ground rock; along with human activities, such as mining, metallurgy, leather process, dyeing industry, use of pesticide and insecticide, etc. [5-8]. Ground water pollution by arsenic is reported to be a greater and serious problem for countries that include the United States, China, Chile, Bangladesh, Taiwan, Mexico, Argentina, Poland, Canada, Hungary, New Zealand, Japan, and India [9-12]. The largest population at risk with known groundwater arsenic contamination is the Bangladeshi followed by the West Bengali in India [13-15]. The US Environmental Protection Agency (EPA) announced that the maximum contaminant level was to be lowered from 50 to 10 μg/L [16, 17]. Similarly, the World Health Organization also recommended lowering the arsenic in drinking water standard to 10 μg/L [18].

Long-term drinking intake of arsenic contaminated waters may cause skin, lung, bladder, and kidney cancer, as well as pigmentation changes, skin thickening (hyperkeratosis) neurological disorders, muscular weakness, loss of appetite, nausea, etc. [15, 19-21]. This differs from acute poisoning, which typically causes vomiting, esophageal and abdominal pain, and bloody "rice water" diarrhea, etc. [15, 19, 20, 22-24].

Various materials were employed in the decontamination of arsenic from the aquatic environment. The aluminum pillared hexadecyltrimethylammonium bromide (HDTMA)- or

Received December 27, 2013 **Accepted** February 07, 2014

†Corresponding Author
E-mail: leesm@kwandong.ac.kr
Tel: +82-33-649-7535 Fax: +82-33-642-7635

alkyldimethylbenzylammonium chloride (AMBA)-sericite was obtained and employed in the remediation of As(III) and As(V) under both the batch and column reactor operations [25]. Inline HDTMA or AMBA modified sericite hybrid materials were employed in the decontamination of arsenic from aqueous solutions under batch reactor operations [26]. Activated carbon obtained by rice hulls or betel nut waste was further modified with manganese to obtain manganese coated activated carbon samples. These manganese modified activated carbons samples were then employed in the removal of As(III) and As(V) from aqueous solutions [27]. Sand is one of the natural filter media widely used in the pretreatment of waste waters, but shows no affinity towards the removal of several heavy metal toxic ions. However, suitable modifications with manganese or iron showed its enhanced applicability in waste water treatment plants, particularly in the removal of several heavy metal/metalloid toxic ions. It is also pointed that the naturally occurring manganese or iron oxides are seemingly immobilized onto the sand surfaces and tend to attenuate the trace metals from soil, sediments and rocks, because of their high sorptive capacities towards several heavy metal toxic ions. Moreover, the manganese or iron oxides possess useful properties, such as high surface area, microporous structure, and available surface functional group –OH, capable of forming strong chemical bonds with several metal ions including phosphate and arsenic [28, 29]. Therefore, because of these properties, the sand samples were modified with manganese or iron oxides and hence widely employed in the removal/speciation of several heavy/radio toxic ions from aqueous solutions [30-35]. Previous studies showed that manganese or iron immobilized sand were employed in the decontamination of Cu(II), Pb(II), Mn(II), Cd(II), Cr(VI), etc. [36-39]. These results prompted us to further assess manganese oxide immobilized natural sand in the remediation of As(III) and As(V) contaminated waters.

2. Materials and Methods

2.1. Materials

Sand was collected from the local river Tlawng at the Sairang site, Aizawl, Mizoram, India. It was washed thoroughly with distilled water followed by 0.2 mol/L HNO_3 to remove any mud, dirt or other adhering impurities. It was again washed with plenty of distilled water and dried. The dried sample was sieved to obtain the 30–60 BSS standard mesh size using a mechanical sieve. The chemicals used for the experiment were manganese nitrate as $Mn(NO_3)_2{\cdot}6H_2O$ (97% Extra Pure; Junsei Chemicals, Tokyo, Japan), sodium meta-arsenite ($NaAsO_2$ GR reagent; HiMedia, Mumbai, India), and sodium arsenate (Na_3AsO_4 GR reagent; Himedia). HNO_3 and NaOH were of AR grade. The water was obtained by purifying the de-ionized with the Millipore water purification system (Milli-Q+).

2.2. Preparation of Immobilized Manganese Dioxide Sand

The IMNS sample is prepared as previously described [40]. In brief, it was obtained by mixing 120 g of cleaned and dried sand (30–60 BSS Standard in size) and 100 mL of 0.05 mol/L manganese nitrate solutions at pH 9.0 in a flask of a rotary evaporator. The mixture was then constantly stirred at 60°C temperature in a rotary evaporator with the slow speed of 30 rpm, till the volume reduced to about 10 mL. The sample was kept in a drying oven at 90°C, till it dried out completely. The sample was then kept at 160°C for approximately 3 hr for complete drying and better coating stability of manganese oxide onto the sand surface. It was cooled at room temperature and again washed with distilled water several times. It was dried in a drying oven at 90°C overnight and stored in a polyethylene bottle. Moreover, the amount of manganese coated onto the surface of sand was obtained by the standard EPA method (US EPA Method 3050B).

2.3. Characterization of Solid Sample

The surface morphology of sand and IMNS materials was obtained by taking the scanning electron microscope (SEM) images of these solids, using a SEM machine (FE-SEM-Model SU-70; Hitachi, Tokyo, Japan) as equipped with energy dispersive X-ray Spectroscopy (EDX) system. X-ray diffraction (XRD) analysis of sand and IMNS samples was obtained using a XRD machine (X'Pert PRO MPD; PANalytical, Almelo, the Netherlands). The data was collected with the scan rate of 0.034 of 2θ illumination and an applied voltage of 45 kV having 35 mA current and using Cu Kα radiation with wavelength 1.5418 Å [38]. The BET specific surface area was obtained using a surface area analyzer (Macsorb HM model-1200 series; Mountech, Tokyo, Japan).

2.4. Stability of the IMNS Solid

The stability of manganese oxide particles aggregated onto the sand surface was assessed in varying solution pH from 2.0 to 11.0. Therefore, 0.5 g of IMNS solid was equilibrated with 100 mL of distilled water at different initial pH values, and then kept in an automatic shaker at 25°C for 24 hr. The solution mixtures were filtered using the 0.45 μm syringe filters and the filtrates were analyzed for total manganese content using an atomic absorption spectrometer (AAS; AA240FS fast sequential atomic absorption spectrometer; Varian Inc., Palo Alto, CA, USA) [38].

2.5. pH_{PZC} Determination of the Solid

The pH_{PZC} (point of zero charge) was defined as the pH value at which the surface carries net zero charge. The acid and base titrations were carried out by taking 5 g of the IMNS sample into 500 mL of distilled water and titrating with 0.1 mol/L of HNO_3 and 0.1 mol/L of NaOH solutions separately [38]. The corresponding pH was recorded using a pH meter (HANNA pH-213 Microprocessor pH meter; HANNA Instruments, Smithfield, RI, USA). The titration data were used to evaluate the pH_{PZC}.

2.6. Effect of pH

Batch experiments were conducted to study the effect of pH on the sorption of As(III) and As(V). As(III) or As(V) solutions 2.0 mg/L were prepared at different pH of 2.0 to 10.0. The pH was obtained by the addition of drops of conc. HNO_3 or conc. NaOH solutions. 0.2 g of IMNS solid was added to 100 mL of each of these sorptive solutions. The solutions were kept in an automatic shaker for 24 hr at 25°C ± 1°C. The solutions were filtered with 0.45 μm syringe filter and the pH was again checked and reported as the equilibrium pH. The filtrates were then subjected to bulk arsenic concentration using the AAS.

The percentage removal of the arsenic was calculated using the Eq. (1):

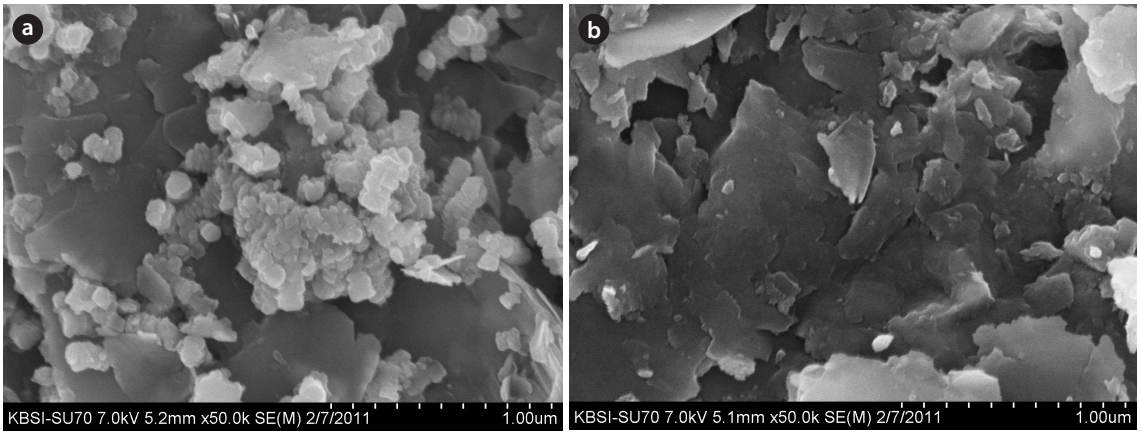

Fig. 1. Scanning electron microscope images of (a) bare sand, and (b) immobilized manganese dioxide natural sand.

$$Removal\ (\%) = \frac{C_0 - C_e}{C_0} \times 100 \quad (1)$$

where C_o and C_e are the initial and bulk sorptive concentrations, respectively.

2.7. Effect of Sorptive Concentration

As(III) or As(V) concentration dependence study was carried out by varying the arsenic concentrations from 1.0 to 20.0 mg/L at a constant equilibrium pH 5.0 and temperature 25°C ± 1°C. The results obtained are reported in terms of sorptive concentration against the percent of total arsenic removal.

2.8. Effect of Background Electrolyte Concentration

The ionic dependence study for the sorption of As(III) or As(V) by IMNS was carried out by varying the background electrolyte concentration from 0.0001 to 0.1 mol/L using $NaNO_3$. The solution pH (4.0) and temperature (25°C ± 1°C) was kept constant throughout the experiments. The remaining sorption procedure was followed as mentioned in the previous section. The results obtained were reported as percent removal as a function of the background electrolyte concentrations.

2.9. Column Studies

The column experiments were performed using a glass column (1 cm inner diameter). The column was packed with 1.0 g of IMNS sample (kept in the middle of the column), 1.0 g each of bare sand (30–60 BSS in size) was placed below and above this, and the rest of the column was packed with glass beads. Sorption solution containing 10.0 mg/L As(III) or As(V) having initial pH 4.0 was pumped upward from the bottom of the column using a Acuflow Series II high pressure chromatograph pump at a constant flow rate of 1.2 mL/min. Effluent solution was collected using a Spectra/Chrom CF-1 Fraction Collector. These collected samples were filtered using a 0.45 μm syringe filter and the total bulk sorptive concentration was measured using AAS.

The breakthrough data obtained were utilized to simulate with the non-linear Thomas equation (2) [41] to optimize the removal capacity of IMNS under the specified column conditions:

$$\frac{C_e}{C_0} = \frac{1}{1 + e^{[K_T(q_0 m - C_0 V)]/Q}} \quad (2)$$

where C_e is the As(III) or As(V) concentration in the effluent (mg/L); C_o is the As(III) or As(V) concentration in the feed (mg/L); K_T is the Thomas rate constant (L/min/mg); q_0 is the maximum amount of the As(III) or As(V), which can be loaded (mg/g) under the specified column conditions; m is the mass of IMNS packed in column (g); V is the throughput volume (L); and Q is the flow rate (L/min) of sorptive solution. A non-linear regression of the breakthrough data was conducted for the least square fitting of the estimation of two unknown parameters, i.e., K_T and q_o [36, 40].

3. Results and Discussion

3.1. Scanning Electron Microscopic Studies

The SEM images of these two samples, i.e., sand and IMNS, are shown in Fig. 1(a) and (b). The image of sand sample clearly shows that the surface is disordered with compact structure, which hardly possesses pores on it. Several aggregated particles of silica, however, appear on the sand surface. On the other hand, the SEM image of IMNS shows that the sand surface is occupied by small sized manganese oxide particles and these particles are distributed over the entire sand surface. Because of these aggregated manganese dioxide particles, the surface shows a heterogeneous structure containing a large number of micropores.

The EDX analysis shows that a distinct peak for the silica, iron, aluminum, and magnesium occurred for both samples, i.e., sand and IMNS (cf. Fig. 1(a) and (b)); whereas, an additional peak of manganese occurred with the IMNS solid, which shows that manganese is aggregated onto the sand surface. The amount of manganese aggregated was found to be 1,446 mg/kg of sand.

3.2. pH_{PZC} Determination of IMNS

The pH_{PZC} of IMNS is found to be 6.28. This value is somewhat higher than the pH_{PZC} of the manganese dioxide as reported as 5.5 [42] and 6.0 [37]. The higher value of pH_{PZC} of IMNS is, perhaps, because of the small size particles of manganese dioxide spread over the sand surface.

3.3. X-Ray Diffraction Studies

X-ray diffraction data obtained for sand and IMNS are presented graphically in Fig. 2. Fig. 2 clearly indicates that the introduction of manganese causes a slight increase in d-values. This indicates that the interlayer of sand structure is propped up slightly. Moreover, possibly due to the amorphous nature of manganese dioxide aggregated on the sand surface, sharp reflections could not be provided of the mineral phase of manganese. These results are in line with the reports given elsewhere, in which the pyrolusite is coated onto the clay surface using very low loading of pyrolusite. The pyrolusite is not detected by the XRD analysis, because there may be inhibition of oxide crystallization or else the oxide nucleated as nanometer particles, which are not detected by XRD [43].

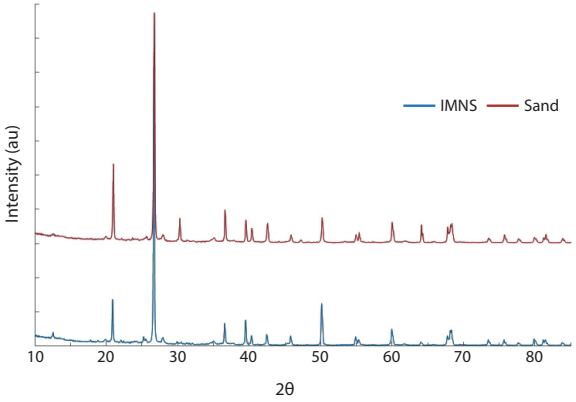

Fig. 2. X-ray diffraction analysis of sand and immobilized manganese dioxide natural sand (IMNS) samples.

3.4. Stability Studies

The stability of immobilized manganese dioxide onto the sand surface is assessed at different pH values and the results show that the manganese strongly occupies the surface of sand within the pH region 3 to 10, since no significant amount of manganese is desorbed into the bulk solution. Whereas, it is slightly unstable at pH 2, since a total of approximately 0.5 mg/L of manganese is leached out from the sand surface. The result suggests that manganese firmly occupies the surface of sand and is likely to have some strong chemical binding with the sorbing species.

The BET multipoint surface area is found to be 8.51 and 11.03 for sand and IMNS, respectively. These results show that IMNS possessed significantly higher specific surface area compared to the bare sand sample.

3.5. Effect of pH

The pH dependence sorption data is an important parameter enabling identification of the mechanism involved at the solid/solution interface. The pH dependence sorption of As(III) or As(V) by the IMNS is shown graphically in Fig. 3. The sorption behavior of these ions as a function of pH is explained by the pH dependent properties of both IMNS surface and arsenic speciation. IMNS solid show the pH_{PZC} of 6.28, i.e., the surface of IMNS is supposed to be positively charged below pH 6.2; and beyond that, it becomes negatively charged (cf. Eq. (3)):

$$\equiv SH_2^+ \underset{pH_{PZC}}{\leftrightarrow} \equiv SH^0 \leftrightarrow \equiv S^- \quad (3)$$

Sorption results show that the increase in pH from approximately 2.0 to 9.0 resulted in the decrease of As(III) removal from 0.288 to 0.154 mg/g and of As(V) from 0.328 to 0.138 mg/g, respectively. This decrease in the amount of As(III) or As(V) by the IMNS is because of the fact that increase of pH led to deprotonation of the IMNS and the surface becomes negatively charged, which hinders the uptake of the negatively charged sorbing species of As(III) or As(V). However, at lower pH conditions the IMNS possesses positive charge, which favors the percent uptake of these two sorbing ions, i.e., As(III) or As(V).

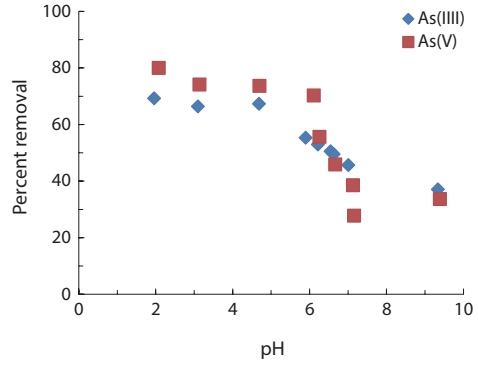

Fig. 3. Effect of pH on the sorption of As(III) and As(V) onto the surface of immobilized manganese dioxide natural sand.

3.6. Effect of Sorptive Concentrations

It is reported that the initial concentration of a sorbing species provided an important driving force to overcome all mass transfer resistances of the sorbing species between aqueous and solid phase [44]. The concentration dependence sorption of As(III) and As(V) by IMNS are shown in Fig. 4. Increasing the sorptive concentration from 1.00 to 25.00 mg/L of As(III) caused an apparently insignificant increase in the amount of As(III) removal, i.e., from 0.124 to 0.180 mg/g compared to the percent of increase in sorptive concentration (cf. from Fig. 4). Similarly, for As(V), the amount adsorbed by the IMNS is increased from 0.138

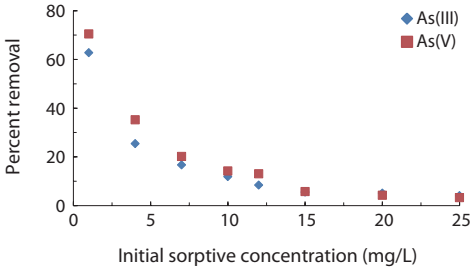

Fig. 4. Effect of sorptive concentration on the sorption of As(III) and As(V) onto the surface of immobilized manganese dioxide natural sand.

to 0.318 mg/g for the similar increase in sorptive concentration, i.e., from 1.0 to 25.0 mg/L. Although the amount of arsenic adsorbed increased with the increase in initial arsenic concentration, the percent removal decreased with the increase of initial concentration. This is because of the fact that at higher concentration of arsenic species, an apparent competition took place towards the limited number of surface active sites [38, 45].

3.7. Equilibrium Modelling

The concentration dependence data was further utilized to model it to the known Freundlich adsorption isotherm. The Freundlich model assumes the sorption occurs on an energetically heterogeneous surface on which the sorbed species interact laterally. The plots are drawn between LogC_e vs. Loga_e for the As(III) and As(V) and it is found that a reasonably good straight line is obtained for these systems. Further, using the fitting equation, the Freundlich constants, i.e., $1/n$ and K_f, along with R^2 values, are evaluated for As(III) and As(V) and tabulated in Table 1. The fractional values of $1/n$ ($0 < 1/n < 1$) obtained for the two systems infer the heterogeneous nature of the solid surface along with the exponential distribution of the adsorption sites [46, 47].

3.8. Effect of Background Electrolytes

The change of ionic strength is one of the important parameters that determine the nature of binding of sorptive ions onto the surface of solids. Outer sphere complexes are predominantly involved with electrostatic interaction and are strongly affected by the ionic strength of aqueous phase; whereas, inner sphere complexes are associated with a strong bond that is chemical in nature and are only weakly affected by the ionic strengths [40, 48]. The results of ionic strength effect on the removal of As(III) and As(V) by IMNS are shown in Fig. 5. It is clearly observed that a change in the background electrolyte concentrations of $NaNO_3$ from 0.0001 to 0.1 mol/L (1,000 times increase) resulted in an insignificant decrease in the removal percent of As(III) or As(V). Quantitatively, increasing the background electrolyte concentration from 0.0001 to 0.1 mol/L $NaNO_3$ caused a decrease in percent uptake from 49.5% to 56.0% (for As(III); i.e., a total decrease by 6.5%) and 57.5% to 60.0% (for As(V); i.e., a total decrease by 2.5%), respectively. These results clearly indicate the sorbing ions are firmly bound onto the solid surface forming 'inner sphere complexes' on the surface of IMNS.

3.9. Column Experiments

The fluidized bed reactor technique is extensively used in the remediation of water contaminated with a variety of toxins [49-53]. The removal of As(III) and As(V) by IMNS is studied using specified column conditions and the results are shown in Fig. 6. These figures clearly demonstrate that a gradual increase of C_e/C_0 occurred with the increase in throughput volume resulting in a breakthrough at 0.6 and 0.7 L for As(III) and As(V) solutions, respectively. The high value of breakthrough volume indicates the higher removal capacity of As(III) and As(V) by IMNS under the dynamic conditions. This further shows that IMNS is a potential and promising material for the removal of As(III) and As(V).

The breakthrough data obtained for As(III) and As(V) is further utilized in the non-linear fitting of Thomas equation (2). The estimated values of the Thomas constants, i.e., the q_0 and K_T, are given in Table 2. The employed solid, i.e., IMNS shows a fairly strong affinity towards As(III) and As(V), since relatively high removal capacity is obtained for the As(III) and As(V).

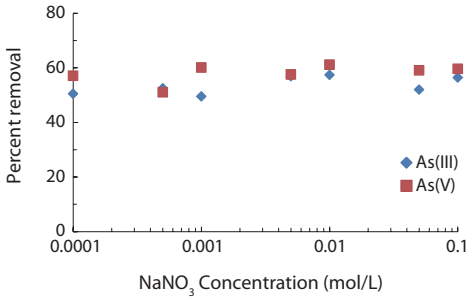

Fig. 5. Ionic strength dependence sorption of As(III) and As(V) by the immobilized manganese dioxide natural sand.

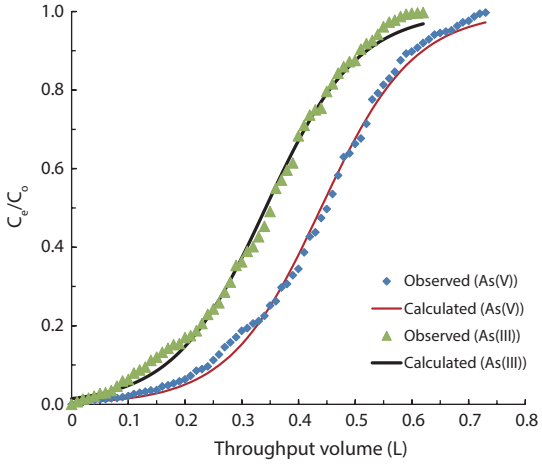

Fig.6. Breakthrough curves obtained for the removal of As(III) and As(V) by immobilized manganese dioxide natural sand solid.

Table 1. Freundlich constants obtained for the adsorption of As(III) and As(V) on IMNS

Sample	1/n	K_f (mg/g)	R^2
As(III)	0.098	1.377	0.886
As(V)	0.187	1.909	0.855

IMNS: immobilized manganese dioxide natural sand.

Table 2. Thomas constants for the removal of As(III) and As(V) by IMNS

Metal ion	q_0 (mg/g)	K_T (L/min/mg)×10^{-3}
As(III)	3.37	1.25
As(V)	4.38	1.23

IMNS: immobilized manganese dioxide natural sand.

4. Conclusions

Small sized manganese dioxide particles are immobilized onto the surface of sand by the wet impregnation process so as to obtain the IMNS. The SEM images of IMNS shows that manganese is very orderly immobilized onto the solid sand surface. The XRD data shows that the interlayers of the sand are propped up with little extent, since an increase in d-values is obtained with IMNS solid. The specific surface area of the solid is obtained, which shows a significant increase in the specific surface area obtained by the immobilization of manganese oxide. The pH_{PZC} (point of zero charge) is found to be 6.28. Further, the IMNS is employed to assess the removal of As(III) and As(V) pollutants from aqueous solutions under the batch and column operations. Batch reactor data shows that an decrease in pH (pH approximately 10.0 to 2.0) and decrease in sorptive concentration (25.0–1.0 mg/L) significantly favors the percent removal of As(III) and As(V) by IMNS. Whereas, the increase in background electrolyte concentrations, i.e., 0.0001–0.1 mol/L $NaNO_3$, causes insignificant change in the percent removal of As(III) or As(V) by IMNS, which indicates that the sorbing ions are forming strong chemical bonds onto the solid surface, and hence, forming an inner sphere surface complexation onto IMNS. Further, column experiments are conducted to enable the efficiency of IMNS under dynamic conditions. The breakthrough data shows that a complete breakthrough is obtained with the throughput volume of 0.6 and 0.7 L for As(III) and As(V), respectively, by IMNS. Further, the non-linear fitting of the breakthrough data to the Thomas equation enables estimation of the loading capacity of the column for As(III) and As(V), which is found to be 3.37 and 4.38 mg/g of IMNS for As(III) and As(V), respectively.

Acknowledgments

This research was supported by the Korea Ministry of Environment as “The Converging Technology Project” (Proposal No. 2013001450001).

References

1. Pink DH. Investing in tomorrow’s liquid gold [Internet]. [place unknown]: Yahoo.com;2006 [cited 2006 Apr 19]. Available from: https://groups.yahoo.com/neo/groups/DESCinvest/conversations/topics/102?var=1&l=1.
2. Sigel H, Sigel A. Metal ions in biological systems. New York: Marcel Dekker; 1985.
3. Martins RJ, Pardo R, Boaventura RA. Cadmium(II) and zinc(II) adsorption by the aquatic moss Fontinalis antipyretica: effect of temperature, pH and water hardness. *Water Res*. 2004;38:693-699.
4. Rout K, Mohapatra M, Mohapatra BK, Anand S. Pb(II), Cd(II) and Zn(II) adsorption on low grade manganese ore. *Int. J. Eng. Sci. Technol*. 2009;1:106-122.
5. Chakravarty S, Dureja V, Bhattacharyya G, Maity S, Bhattacharjee S. Removal of arsenic from groundwater using low cost ferruginous manganese ore. *Water Res.* 2002;36:625-632.
6. Smedley PL, Kinniburgh DG. A review of the source, behaviour and distribution of arsenic in natural waters. *J. Appl. Geochem*. 2002;17:517-568.
7. Bhumbla DK, Keefer RF. Arsenic mobilization and bioavailability in soils. In: Nriagu JO, ed. Arsenic in the environment: Part I. Cycling and characterization. New York: John Wiley & Sons; 1994. p. 51-82.
8. Kim MJ, Nriagu J, Haack S. Arsenic species and chemistry in groundwater of southeast Michigan. *Environ. Pollut*. 2002;120:379-390.
9. Burkel RS, Stoll RC. Naturally occurring arsenic in sandstone aquifer water supply wells of Northeastern Wisconsin. *Groundw. Monit. Remediat.* 1999;19:114-121.
10. Cebrian ME, Albores A, Aguilar M, Blakely E. Chronic arsenic poisoning in the north of Mexico. *Hum. Toxicol.* 1983;2:121-133.
11. Dhar RK, Biswas BK, Samanta G, et al. Groundwater arsenic calamity in Bangladesh. *Curr. Sci.* 1997;73:48-59.
12. Karim MM. Arsenic in groundwater and health problems in Bangladesh. *Water Res*. 2000;34:304-310.
13. Das D, Chatterjee A, Mandal BK, Samanta G, Chakraborti D, Chanda B. Arsenic in ground water in six districts of West Bengal, India: the biggest arsenic calamity in the world. Part 2. Arsenic concentration in drinking water, hair, nails, urine, skin-scale and liver tissue (biopsy) of the affected people. *Analyst* 1995;120:917-924.
14. Chatterjee A, Das D, Mandal BK, Chowdhury TR, Samanta G, Chakraborti D. Arsenic in ground water in six districts of West Bengal, India: the biggest arsenic calamity in the world. Part 1. Arsenic species in drinking water and urine of the affected people. *Analyst* 1995;120:643-650.
15. Jain CK, Ali I. Arsenic: occurrence, toxicity and speciation techniques. *Water Res*. 2000;34:4304-4312.
16. An B, Steinwinder TR, Zhao D. Selective removal of arsenate from drinking water using a polymeric ligand exchanger. *Water Res.* 2005;39:4993-5004.
17. Wang L, Fields KA, Chen AS. Arsenic removal from drinking water by ion exchange and activated alumina plants. Cincinnati: National Risk Management Research Laboratory, Office of Research and Development, US Environmental Protection Agency; 2000.
18. Smedley PL, Kinniburgh DG. United Nations synthesis report on arsenic in drinking water. Geneva: World Health Organization; 2001.
19. Kipling MD. Arsenic. In: Lenihan JM, Fletcher WW, eds. The chemical environment. Glasgow: Academic Press; 1977. p. 93-120.
20. World Health Organization. Arsenic (Environmental Health Criteria 18). Geneva: World Health Organization; 1981.
21. Mandal BK, Suzuki KT. Arsenic round the world: a review. *Talanta* 2002;58:201-235.
22. DeSesso JM, Jacobson CF, Scialli AR, Farr CH, Holson JF. An assessment of the developmental toxicity of inorganic arsenic. *Reprod. Toxicol.* 1998;12:385-433.
23. Duker AA, Carranza EJ, Hale M. Arsenic geochemistry and health. *Environ. Int*. 2005;31:631-641.
24. Ng JC, Wang J, Shraim A. A global health problem caused by arsenic from natural sources. *Chemosphere* 2003;52:1353-1359.
25. Tiwari D, Lee SM. Novel hybrid materials in the remediation of ground waters contaminated with As(III) and As(V). *Chem. Eng. J*. 2012;204-206:23-31.
26. Lee SM, Tiwari D. Organo-modified sericite in the remediation of an aquatic environment contaminated with As(III) or As(V). *Environ. Sci. Pollut. Res.* 2014;21:407-418.
27. Lalhmunsiama, Tiwari D, Lee SM. Activated carbon and

manganese coated activated carbon precursor to dead biomass in the remediation of arsenic contaminated water. *Environ. Eng. Res*. 2012;17(S1):S41-S48.
28. Al-Sewailem MS, Khaled EM, Mashhady AS. Retention of copper by desert sands coated with ferric hydroxides. *Geoderma* 1999;89:249-258.
29. Gadde RR, Laitinen HA. Heavy metal adsorption by hydrous iron and manganese oxides. *Anal. Chem*. 1974;46:2022-2026.
30. Han R, Zou W, Zhang Z, Shi J, Yang J. Removal of copper(II) and lead(II) from aqueous solution by manganese oxide coated sand: I. Characterization and kinetic study. *J. Hazard. Mater.* 2006;137:384-395.
31. Han R, Lu Z, Zou W, Daotong W, Shi J, Jiujun Y. Removal of copper(II) and lead(II) from aqueous solution by manganese oxide coated sand: II. Equilibrium study and competitive adsorption. *J. Hazard. Mater*. 2006;137:480-488.
32. Deschamps E, Ciminelli VS, Holl WH. Removal of As(III) and As(V) from water using a natural Fe and Mn enriched sample. *Water Res.* 2005;39:5212-5220.
33. Lee CI, Yang WF, Hsieh CI. Removal of copper(II) by manganese-coated sand in a liquid fluidized-bed reactor. *J. Hazard. Mater*. 2004;114:45-51.
34. Ahammed MM, Meera V. Iron hydroxide-coated sand filter for household drinking water from roof-harvested rainwater. *J. Water Supply Res. Technol*. 2006;55:493-498.
35. Yang JK, Song KH, Kim BK, Hong SC, Cho DE, Chang YY. Arsenic removal by iron and manganese coated sand. *Water Sci. Technol*. 2007;56:161-169.
36. Lee SM, Kim WG, Laldawngliana C, Tiwari D. Removal behavior of surface modified sand for Cd(II) and Cr(VI) from aqueous solutions. *J. Chem. Eng. Data* 2010;55:3089-3094.
37. Lee SM, Tiwari D, Choi KM, Yang JK, Chang YY, Lee HD. Removal of Mn(II) from aqueous solutions using manganese-coated sand samples. *J. Chem. Eng. Data* 2009;54:1823-1828.
38. Tiwari D, Laldanwngliana C, Choi CH, Lee SM. Manganese-modified natural sand in the remediation of aquatic environment contaminated with heavy metal toxic ions. *Chem. Eng. J*. 2011;171:958-966.
39. Lee SM, Laldawngliana C, Tiwari D. Iron oxide nano-particles-immobilized-sand material in the treatment of Cu(II), Cd(II) and Pb(II) contaminated waste waters. *Chem. Eng. J*. 2012;195-196:103-111.
40. Tiwari D, Yu MR, Kim MN, et al. Potential application of manganese coated sand in the removal of Mn(II) from aqueous solutions. *Water Sci. Technol*. 2007;56:153-160.
41. Thomas HC. Heterogeneous ion exchange in a flowing system. *J. Am. Chem. Soc*. 1944;66:1664-1666.
42. Koulouris G. Dynamic studies on sorption characteristics of 226Ra on manganese dioxide. *J. Radioanal. Nucl. Chem.* 1995;193:269-279.
43. Boonfueng T, Axe L, Xu Y. Properties and structure of manganese oxide-coated clay. *J. Colloid. Interface Sci.* 2005;281:80-92.
44. Malkoc E. Ni(II) removal from aqueous solutions using cone biomass of Thuja orientalis. *J. Hazard. Mater*. 2006;137:899-908.
45. Tiwari D, Kim HU, Lee SM. Removal behaviour of sericite for Cu(II) and Pb(II) from aqueous solutions: batch and column studies. *Sep. Purif. Technol*. 2007;57:11-16.
46. Benes P, Majer V. Trace chemistry of aqueous solutions. Amsterdam: Elsevier; 1980.
47. Mishra SP, Tiwari D, Dubey RS, Mishra M. Biosorptive behavior of casein for Zn^{2+}, Hg^{2+} and Cr^{3+} effects of physico-chemical treatments. *Bioresour. Technol.* 1998;63:1-5.
48. Sparks DL. Environmental soil chemistry. San Diego: Academic Press; 1995.
49. Harns WD Jr, Robinson RB. Softening by fluidized-bed crystallizers. *J. Environ. Eng.* 1992;118:513-529.
50. Aktor H. Continuous high rate removal of chromate in a fluidized bed without sludge generation. *Water Sci. Technol.* 1994;30:31-40.
51. Nielsen PB, Christensen TC, Vendrup M. Continuous removal of heavy metals from FGD wastewater in a fluidised bed without sludge generation. *Water Sci. Technol*. 1997;36:391-397.
52. Scholler M, van Dijk JC, Wilms D. Recovery of heavy metals by crystallization. *Met. Finish*. 1987;85:31-34.
53. Wilms D, Vercamst K, van Dijk JC. Recovery of silver by crystallization of silver carbonate in a fluidized bed reactor. *Water Res.* 1992;26:235-239.